N. Feito, J. López-Puente, C.Santiuste, H. Miguélez (2014). Numerical prediction of delamination in CFRP drilling. *Composite Structures*, 108, February, pp. 677-683. Avalaible in http://dx.doi.org/10.1016/j.compstruct.2013.10.014

Numerical prediction of delamination in CFRP drilling

N. Feito [a], J. López-Puente [b], C. Santiuste [b], M.H. Miguélez [a,*]

[a] Department of Mechanical Engineering, Universidad Carlos III de Madrid, Avda. Universidad 30, 28911 Leganés, Madrid, Spain
[b] Department of Continuum Media and Structural Analysis, Universidad Carlos III de Madrid, Avda. Universidad 30, 28911 Leganés, Madrid, Spain

Abstract: Delamination is one of the undesired effects of machining using non appropriate cutting parameters or worn drill. Finite element modeling of drilling of Carbon Fiber Reinforced Polymer (CFRP) composites is an interesting tool for damage prediction. Recently, complete modeling of the process including the rotatory movement of the drill, penetration in the composite plate and element erosion has been developed in the scientific literature. Computational cost of these complex models is a great disadvantage when comparing them with simplified models that consider the drill acting like a punch that pierces the laminate. In this paper both complete and simplified models were developed and compared in terms of delamination prediction. The simplified model, presenting reduced computational cost, slightly overestimates the delamination factor when compared with the complex model. The influence on delamination of thrust force, clamping area at the bottom surface of the laminate and the stacking sequence is studied using the simplified model.

Keywords: CFRPs, Drilling, Delamination, Modeling.

1. Introduction

Carbon Fiber Reinforced Polymer (CFRP) composites combine fatigue and corrosion resistance, light weight and high specific stiffness and strength. These properties make CFRPs suitable for a wide range of high responsibility applications. Manufacturing and final assembly of the components commonly requires machin-ing processes needed to achieve dimensional tolerances and assembly specifications. CFRP composites are difficult to cut mate-rials due to the presence of hard fibers. On the other hand, they are vulnerable to the generation of damage during processing: delam-ination, fiber pull-out and matrix thermal degradation are usually observed when cutting parameters are not properly defined. Con-ventional machining operations of CFRPs, mainly milling and dril-ling, should be designed to be productive processes ensuring the quality of the resultant component. The surface quality plays an important role in the improvement of fatigue life of composite components [1].

Drilling operations are required before mechanical joining of the CFRP components [2]. A significant percentage of the compo-nent rejection in aircraft manufacturing is due to delamination in-duced during drilling. Delamination is one of the undesired effects of machining using non appropriate cutting parameters or worn drill and has received extensive attention in the literature. A brief summary of significant contributions is provided below.

* Corresponding author. Tel.: +34 916249402.
E-mail address: mhmiguel@ing.uc3m.es (M.H. Miguélez).

Davim et al. [3] analyzed the influence of cutting parameters and the matrix on the specific cutting force, delamination factor and surface roughness. The feed rate was found to be the most influencing parameter on delamination factor.

Abrao et al. [4] checked the influence of tool geometry and cutting parameters on delamination during drilling of glass FRP. It was shown the strong influence of the drill geometry in competition with the thrust force, commonly assumed to be the most influencing factor. The authors demonstrated that the drill corresponding to the highest thrust force caused the second smallest delaminated area because of its favorable geometry.

Delamination factor after drilling FRP laminates was evaluated in [5] using a digital analysis. The digital analysis showed its suitability for control of drilling induced damage in CFRPs. This technique has been also applied to damage control in high speed drilling of glass FRP [6]. Delamination decreased as the cutting speed was increased within the cutting range tested, probably due to the enhanced cutting temperature with spindle speed, leading to increased softening of the matrix and less delamination.

The most important contributions in the field of composite drilling are summarized in a recent review [7] including techniques, tools and operations developed to minimize the occurrence of delamination.

The measurement of damage is expensive and sometimes requires destructive techniques, thus it is desirable to develop simulation tools able to predict damage mechanisms induced during machining. However, only few works in scientific literature deal with modeling of cutting processes in composite. These works are mostly focused on two dimensional (2D) approaches to

orthogonal cutting although recently, some attempts in three dimensional (3D) modeling have been published. Of course, 3D analysis is required for drilling analysis. Main advantage of 2D modeling relies on the reduced computational cost, however it is not possible to reproduce neither out-of-plane failure mechanisms nor simulating quasi-isotropic laminates. 2D modeling has been developed by different authors, examples can be found in [8–12] analyzing, between other factors, the influence of fiber orientation, cutting parameters and material properties in orthogonal machining of LFRP composites.

The validity of the hypothesis assumed in 2D approaches to LFRP composite cutting has been analyzed in [13,14]. Out-of-plane failure in orthogonal cutting of composites was studied using a three dimensional model based on finite elements. The influence of stacking sequence on the generation of damage was demon-strated and delamination was predicted using cohesive interactions.

Finite element modeling of the complex drilling process has recently achieved in [15,16]. In these works drilling of CFRP was successfully reproduced including drill penetration in the workpiece, material failure and elements erosion. Good agreement between measured and predicted torque, thrust force and delamination extension was shown.

Previously, simplified models of CFRP drilling were developed, having the advantage of most reduced computational cost. Modeling of drilling processes involves elevated difficulty, because of the need of simulating drill rotation and feed movement. Common assumption in simplified models considers the drill acting like a punch that pierces the laminate, see for instance [17,18]. This was the approach used by Durao et al. [19] and Singn et al. [20] when studying GFRP drilling; they showed the influence of the drill point angle in the induced damage.

Main contributions in the field of composite machining modeling have been summarized in a recent work [21].

The interest of modeling drilling processes is clear due to the importance of this operation for industry. The available simulation tools assumes on one hand; simplifying hypothesis (treating the problem as a punching process, with efficient computational cost and reduced geometrical complexity); or model the drilling process rigorously simulating rotation and feed movement of the tool (including penetration of the drill in the workpiece and element erosion, leading to elevated computational cost). The implementation of machining models in industry is still a challenge, probably because of the complexity of the simulation tools and the computational time required. The availability of simple models leading to reasonably predictions could help in the wide implementation of simulation tools in industry.

In this paper a comparison between the predictions provided by a simplified and a complete drill model based on finite element is provided. The aim is giving an overview of the main advantages of both types of modeling, analyzing their accuracy when predicting delamination and study the influence of some parameters involved in delamination. The paper is structured in the present introduction, followed by models description and validation, results and discussion and main conclusions derived from the study.

2. Numerical models and validation

Two numerical models simulating respectively complete drilling and simplified punching of tape laminate, were developed using the commercial finite element code ABAQUS.

A scheme of the models, showing boundary conditions, is presented in Fig. 1. In the simplified model the drill acts like a punch pushing the laminate (two stages of the drill penetration are simulated), see Fig. 1a. The complete model reproduces the complex 3D process with rotary and feed movement (Fig. 1b). The drill and the laminate characteristics were the same for both models and were obtained from Ref. [15] for model validation. Both models include restriction to displacement in z direction in the base of the workpiece except inside a circumference with diameter 16 mm where the z displacement is free. On the other hand displacements were not allowed in the contour of the workpiece [15].

2.1. Drill and workpiece description

The main characteristics of the drill and the workpiece, common for both complete and simplified models, are presented below.

The drill was assumed to be rigid, with diameter equal to 3 mm and the tip angle equal to 120°.

The workpiece was similar to that used for experimental validation (see [15]): CFRP composite (UD T300/LTM45-EL) composed of tape plies with thickness 2 mm consisting of 16 plies with stacking sequence $[0_4/90_4]_s$ (being each ply 0.125 mm thick). Each ply was modeled at the zone close to the drill entrance using solid elements C3D6R with six nodes (1 element along the thickness). The use of wedge elements (prismatic element with triangular section) minimizes the dependence of the results with mesh orientation in the laminate plane. Minimum element size was 0.25 mm. Far from to the drill entrance zone hexagonal elements C3D8R with 8 nodes and reduced integration were used, with minimum element size around 1 mm [22].

The anisotropic composite was modeled using an elastic behavior up to failure. Elastic properties of the composite are presented in Table 1, where E_1 and E_2 are respectively longitudinal and transverse modulus, G_{12} and G_{23} are respectively in-plane and out-of-plane shear modulus and v_{12} is major Poisson's ratio.

The intralaminar failure model was based on Hou criteria [23] and was introduced through a user subroutine VUMAT for the

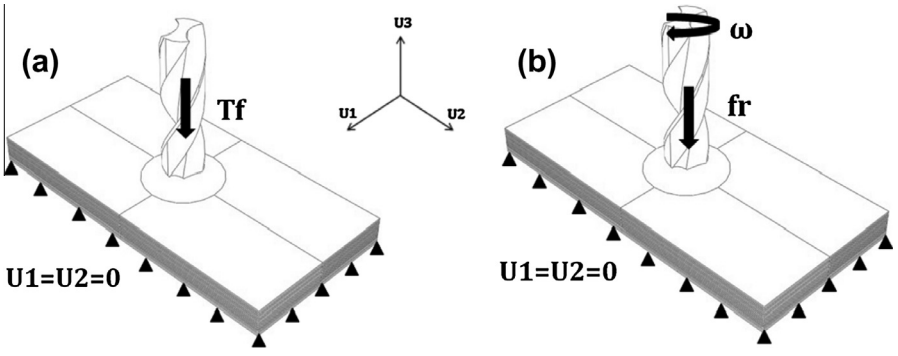

Fig. 1. (a) Scheme of simplified model (*Tf* trust force). (b) Scheme of the complete model (*w* rotation speed, *fr* feed rate).

Table 1
Material ply properties [15] and critical values of the strain for element deletion.

Property	Value
ρ (kg/m^3)	1600
E_1 (GPa)	127
E_2 (GPa)	9.1
G_{12} (GPa)	5.6
G_{23} (GPa)	4
ν_{12}	0.31
X_t (MPa)	2720
X_c (MPa)	1690
Y_c (MPa)	214
S_{12} (MPa)	115
ε_{1c}	0.0525
ε_{2c}	0.0525
ε_{3c}	0.07

carbon/epoxy laminate. This model has been used widely in the literature (see for instance [24,25]).

This model considers three different types of damage (fiber failure and matrix cracking and crushing; Eqs. (1)–(3) defining different damage variables d (stress dependent) ranging from 0 (no damage) to 1 (fully broken).

$$\text{Fiber failure}: \quad d_f^t = \left(\frac{\sigma_{11}}{X_t}\right)^2 + \left(\frac{\tau_{12}}{S_{12}}\right)^2 \leqslant 1 \tag{1}$$

$$\text{Matrix cracking}: \quad d_m^t = \left(\frac{\sigma_{22}}{Y_t}\right)^2 + \left(\frac{\tau_{12}}{S_{12}}\right)^2 \leqslant 1 \tag{2}$$

$$\text{Matrix crushing}: \quad d_m^c = \frac{1}{4}\left(\frac{-\sigma_{22}}{S_{12}}\right)^2 + \left(\frac{Y_c^2\sigma_{22}}{4S_{12}^2 Y_c}\right)^2 - \left(\frac{\sigma_{22}}{Y_c}\right) + \left(\frac{\tau_{12}}{S_{12}}\right)^2 \leqslant 1 \tag{3}$$

where σ_{11} and σ_{22} are the stress in fiber and transverse direction respectively, and σ_{12} the in-plane shear stress. Constants X_t and Y_t are tensile strengths in longitudinal and transverse directions respectively; Y_c is the transverse compressive strength; and S_{12} is the in-plane shear strength. The values of these constants are summarized in Table 1. When one of the damage variables reaches the value 1, all the stress components that appear in the equation are set to zero. The stresses on a damaged element drop to values close to zero and hence large deformations appear. These elements do not contribute to the strength or the stiffness of the composite, but they can cause lack of convergence during simulation and instability problems. Erosion criterion based on maximum strain criteria was implemented in the VUMAT subroutine to remove the distorted elements. After each time increment the longitudinal strains (ε_{11}, ε_{22} and ε_{33}) were evaluated, and the element was removed if one of the strains reached a critical value (ε_{1c}, ε_{2c} and ε_{3c}) provided in Table 1.

The inter-laminar failure was modeled using cohesive elements. Small thickness was assigned to the interface (5 μm) in order to improve numerical behavior when elevated deformations are reached during calculation. Meshing strategy in the plane 1–2 was the same as that used in the ply, with one element along the thickness (direction 3).

The delamination modeling requires the establishment of a damage initiation criteria and a damage evolution law. The onset of delamination is commonly defined using criteria based on normal and shear stresses (Eq. (4)) [23,26]:

$$\left(\frac{\sigma_{33}}{t_n}\right)^2 + \left(\frac{\sigma_{13}}{t_s}\right)^2 + \left(\frac{\sigma_{23}}{t_t}\right)^2 \geqslant 1 \tag{4}$$

where t_n, t_s and t_t are the strengths of the cohesive interface in the normal and in the two shear directions respectively. This criterion is applied if one of the following conditions is reached:

$$\sigma_{33} \geqslant Z_t \quad \text{or} \quad \sqrt{\sigma_{12}^2 + \sigma_{13}^2} \geqslant S_{23} \tag{5}$$

where Z_t is the laminate strength under tension in the through thickness direction and S_{23} is the laminate shear strength.

Concerning the damage evolution, the most used laws are based on the energy dissipation because of the damage process (fracture energy). Examples of these laws are Benzeggagh–Kenane (BK) [27] and potential laws [21] expressed respectively with the following equations:

$$G_n^C + \left(G_s^C - G_n^C\right)\left\{\frac{G_S}{G_T}\right\}^\eta = G^C \tag{6}$$

$$\left(\frac{G_n}{G_n^C}\right)^\alpha + \left(\frac{G_s}{G_s^C}\right)^\alpha + \left(\frac{G_t}{G_t^C}\right)^\alpha = 1 \tag{7}$$

where G_n, G_s and G_t are the released rate energy in the normal and in the two shear directions respectively; G_n^C, G_s^C and G_t^C are the critical values of the released rate energy, being α y η parameters of the model. The models of initiation and evolution of damage have been implemented in ABAQUS using cohesive elements provided in the FE code and widely used in different applications [28–30].

In the present work, a quadratic nominal stress criterion given in Eq. (4) has been used. The damage evolution is simulated through a potential law based on energy, see Eq. (7) with $\alpha = 1$. Element erosion was produced as the failure criterion was reached. The response of the cohesive elements is governed by a traction-separation law illustrated in Fig. 2 for failure mode type I. The definition of this law requires the specification of the linear elastic behavior by means of the stiffness in the normal and in the two shear directions (K_{nn}, K_{ss} and K_{tt}), the interface resistance in each direction (t_n, t_s and t_t) and the damage evolution through the critical released rate energy (G_n^C, G_s^C and G_t^C). The properties related with the cohesive elements are summarized in the Table 2.

The interaction between workpiece and tool was modeled using the algorithm surface–node surface contact available in ABAQUS/Explicit. The contact was defined between the drill surface and the composite plate nodes in the region adjacent to the contact area. In addition, a self-contact condition was used to avoid penetration between eroded composite elements. A constant coefficient of friction equal to 0.3 at the tool/workpiece interface was assumed.

2.2. Characteristics of the complete model

This model involved a dynamic analysis including geometric non-linearity and large deformations options. The problem was solved using an explicit integration scheme (ABAQUS/Explicit). A compromise between accuracy and computational cost was achieved when selecting the element size (previously commented) directly involved in time step.

The rotatory movement of the drill around the y axis at constant spindle speed and the feed rate in direction y were imposed. A

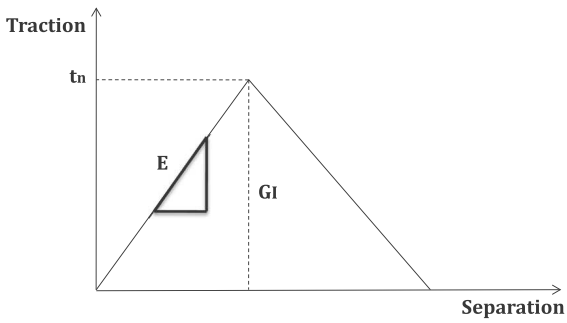

Fig. 2. Behaviour of cohesive elements (E, elastic modulus; t_n, peak value of nominal stress when deformation is purely normal to interface; G_I, instantaneous fracture energy in normal direction).

Table 2
Properties of the cohesive elements.

K_{nn}	$K_{ss} = K_{tt}$	t_n	$t_s = t_t$	G_n^c	$G_s^c = G_t^c$
2 GPa	1.5 GPa	60 MPa	90 MPa	0.287 N/mm	1.833 N/mm

section of the drilled hole simulated with the complete model is presented in Fig. 3, showing the entrance and the exit of the drill.

The cutting parameters were stated equal to those provided in Ref. [15] used for validation. The rotary velocity was equal to 2500 rpm and feed rate was equal to 2.5, 5 and 8.3 mm/s.

The calculation time for simulation ranged from 4 days to 3 weeks in a workstation with 16 CPU.

2.3. Characteristics of the simplified model

This model involved a dynamic analysis carried out using also an explicit integration scheme (ABAQUS/Explicit). No rotation was imposed to the drill. A constant thrust force (obtained from the complete model previously validated) was applied at the top of the drill, corresponding to the level of penetration of the drill at the stage simulated.

The elements corresponding to the pre-drilled volume were removed from the model and the drill contacted the workpiece at a depth equal to H (see Fig. 4). Two stages of the drill penetration across the workpiece were simulated: H equal to 1 mm and 1.625 mm (corresponding respectively to 8 and 13 plies drilled respectively). First stage corresponds to the maximum level of thrust force observed experimentally and also in simulations with the complete model. The second stage was selected because only few plies are not drilled and the origin of delamination is commonly observed close to the drill exit.

Efficient computation was achieved for simulation in the order of several min of calculation time in a workstation with 16 CPU.

3. Model validation and results

3.1. Validation

The complete model was validated through the comparison with experimental results provided in a recent work [15] dealing with drilling of tape carbon–epoxy LFRP composite.

The model was validated in terms of delamination factor at the entrance of the drill, torque and thrust force. Delamination factor was calculated as the ratio between maximum diameter of delaminated area and the nominal diameter of the drill. Fig. 5a–c shows reasonable accuracy when predicting these parameters.

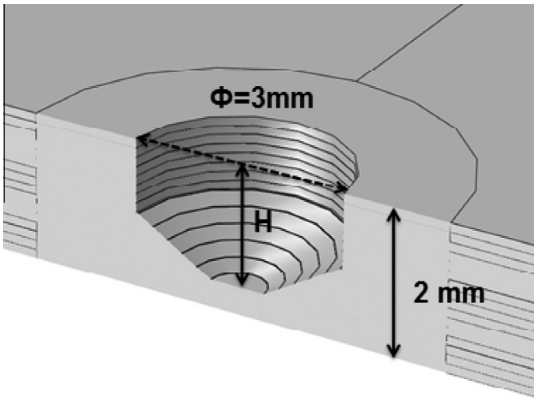

Fig. 4. Scheme of the pre-drilled hole in the simplified model.

3.2. Comparison between simplified and complete model

The simplified model needs as an input the value of thrust force (obtained at the drill penetration simulated) and main output is the prediction of the delaminated area. The complete model also provides delamination but the input data are rotary velocity and feed rate. Fig. 6a and b shows delamination factor predicted with both models for both stages of penetration considered (clamping was applied in direction z at the bottom of the plate, except of a free circular surface with diameter 16 mm).

It is possible to observe the overestimation of delamination factor predicted with the simplified model; in particular it is slightly larger than that obtained with the complete model. It is important to highlight this result: the simplified model is conservative when predicting delamination.

During drill penetration it is also interesting to analyze intralaminar damage. Matrix and fiber failure result in element erosion as the drill penetrates though the workpiece. The intralaminar damage was observed beneath the drill tip as it advances though the composite or pushes it, depending on the model considered. The intralaminar damage is observed in zones with lower diameter than the drill. Thus the damaged zone is eroded as the drill penetrates the composite plate. In consequence only the inter-laminar damage, i.e. delamination is analyzed.

3.3. Influence of thrust force

The simplified model was applied to the analysis of the influence of thrust force, results are presented in Fig. 7. The force was

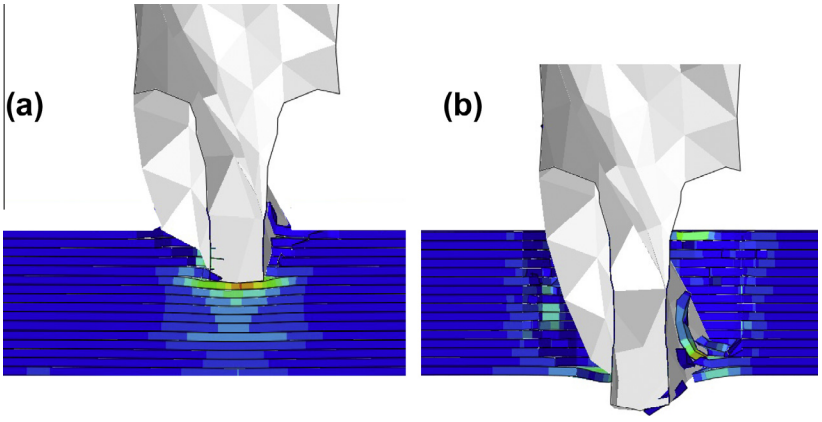

Fig. 3. Section of the hole during penetration of the drill simulated with complete model: (a) entrance and (b) exit of the drill.

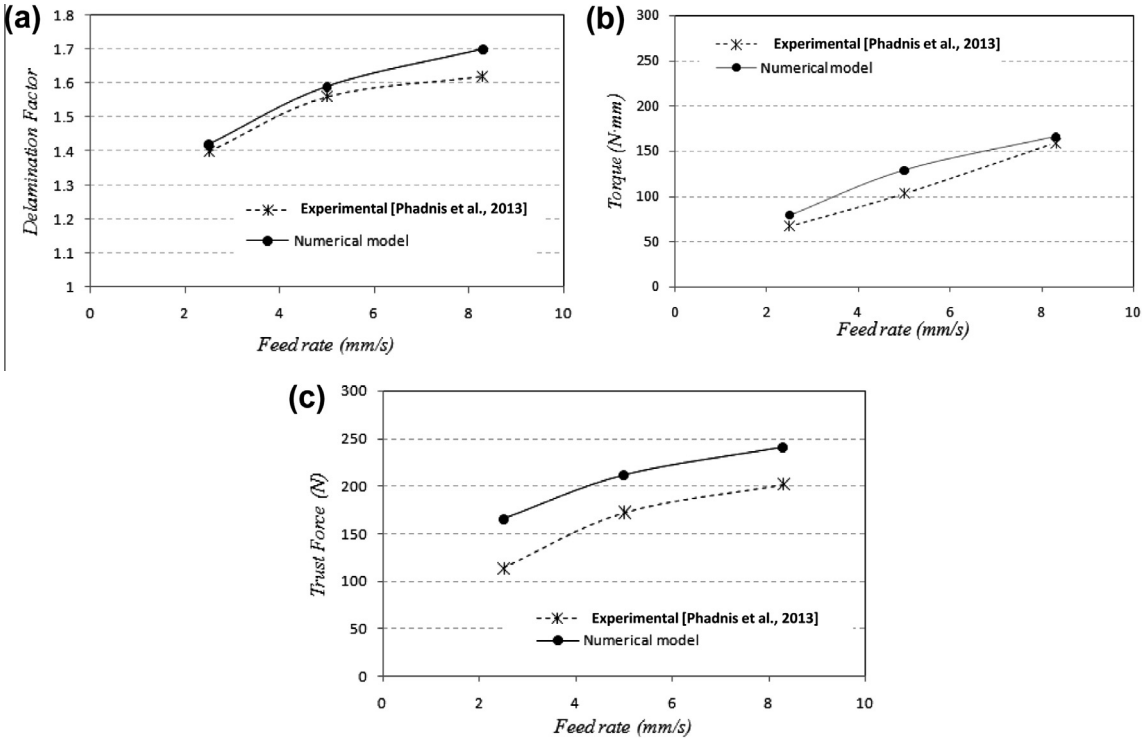

Fig. 5. Validation of complete model though the comparison with experimental data in [15] (a) delamination factor at the entrance of the drill; (b) predicted and experimental torque; and (c) predicted and experimental thrust force.

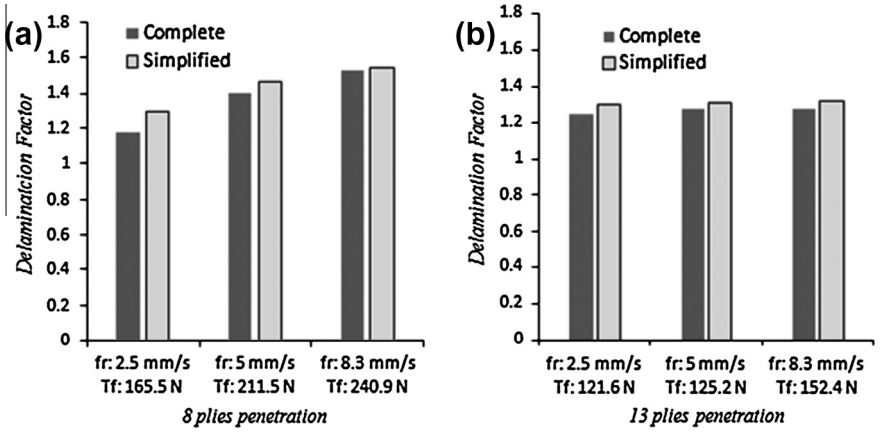

Fig. 6. Predicted and experimental delamination factor, (a) penetration of the drill trough 8 plies and (b) penetration of the drill trough 13 plies.

varied from 50 to 500 N showing strong influence of the force on delamination factor in the range 120–250 N being the factor increased from 1.15 to 1.55.

At low values of the thrust force the value of delamination factor is close to 1 in agreement with other authors showing a minimum value for delamination onset: below this threshold no delamination is produced [7].

It is possible to observe a plateau for values of the thrust force higher than 250 N. The maximum value of delamination factor was compared with that obtained in a complete perforation of the plate. Simulation of complete perforation was achieved with a simple modification of the complete model: rotation of the drill was not considered and the drill pierces the plate at constant feed rate (perforation velocity was stated equal to 150 mm/s). The delamination factor obtained in the complete perforation at constant velocity (D around 1.57) was similar to that obtained at elevated thrust forces being an upper limit of delamination during drilling.

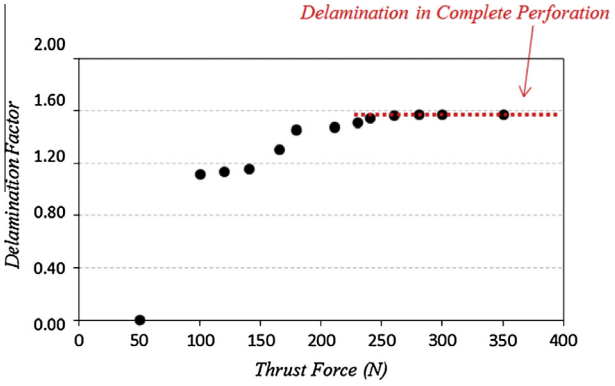

Fig. 7. Influence of thrust force on delamination factor, maximum values tending to delamination observed in complete perforation of the plate.

This is an interesting result since simulations of drilling has an elevated computational cost, while the simulation of perforation at high velocity is more efficient.

3.4. Influence of clamping

The influence of clamping diameter was analyzed using the simplified model. The use of clamping is commonly desired in industry when drilling plates of composite in order to diminish delamination. Sometimes the configuration of the components does not allow drilling with clamping consisting of a posterior metal plate or similar. To study the effect of the clamping the displacement in direction z was restricted in the base of the workpiece except of a circle of diameter equal to 3 mm (drill diameter), 6 mm and 16 mm (16 mm is the nominal value used for validation and for the analysis described in previous sections). Also the case without clamping was analyzed.

Input forces corresponds with the maximum level of thrust force (small value of penetration $H = 1$ mm) obtained for each case of feed velocity analyzed ($F_1 = 165.5$ N, $F_2 = 211.5$ N and $F_3 = 240.9$ N respectively).

All cases analyzed (see Fig. 8) showed variations of delamination factor around 20% when comparing the most restrictive clamping with the highest free area. The effect of clamping can be considered negligible for values of the free area higher than 15 mm and equivalent to free surface.

3.5. Influence of stacking sequence

The laminate studied in the paper is based on the stacking sequence $[0_4/90_4]_s$. It is interesting to test the influence of stacking sequence on delamination, in fact most used laminates are based on a quasi-isotropic configuration. Industrial applications commonly involve multi-axial load states and the superior behavior of quasi-isotropic laminates recommends the use of these stacking sequences. Two different configurations of quasi-isotropic laminates ($[45/-45/0/90]_4$ and $[90/0/45/-45]_4$) were simulated and compared for the different levels of thrust force considered ($F_1 = 165$ N, $F_2 = 211$ N and $F_3 = 241$ N respectively). Quasi-isotropic laminates showed better behavior concerning delamination factor. Differences around 20% (see Fig. 9) are observed when comparing delamination factor in quasi-isotropic laminate and the reference laminate.

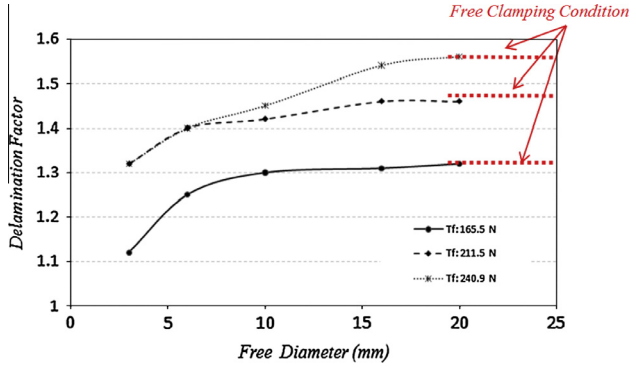

Fig. 8. Delamination factor vs. diameter of the free surface at the bottom of the plate in the simplified model.

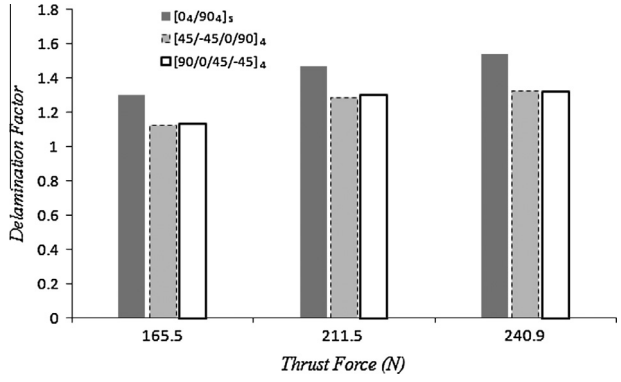

Fig. 9. Influence of stacking sequence on delamination factor.

4. Conclusions

A numerical analysis of CFRP composite drilling is presented in this paper. Modeling was developed using two approaches. Firstly a complete model of drilling, including feed and rotation movements of the drill was developed. Secondly a simplified model, assuming that the drill acts like a punch was done. Both models were compared in terms of factor of delamination prediction. Simplified model slightly overestimates the value of delamination factor, giving a conservative prediction of damage. This result is especially significant when the complexity and the calculation cost of both models are compared. Simplified simulations can be solved in several minutes while the complete model needs several days; this methodology could be considered when designing drilling processes with different drill geometries and cutting parameters. The implementation of numerical models in industry in order to help designing process requires simple and fast simulation tools.

Simplified model was used to study the influence of several factors involved in the drilling process. First of all, the influence of thrust force has been analyzed. It is well known the increasing trend in delamination factor as the force is increased. In this paper it is found a plateau limiting this increment of delamination factor at high enough thrust forces. The maximum level of delamination is coincident with that induced by complete piercing perforating the composite plate with a punch with similar geometry as the drill. Although perforation is not commonly used in hole manufacturing in composites, the delamination factor in this process can be used as an upper limit for the conventional drilling, giving valuable information for the designer.

The influence of clamping has been studied founding significant increment in delamination factor when the diameter of the free surface ranged from the value equal to the drill diameter to higher values up to five times the drill diameter. For higher values negligible influence of the clamping is observed.

Finally the simplified model was used to simulate other stacking sequences corresponding to laminates $[45/-45/0/90]_4$ and $[90/0/45/-45]_4$. The quasi-isotropic laminates presented similar delamination factor, in both cases lower than that exhibited by the laminate $[0_4/90_4]_s$.

Acknowledgement

The authors acknowledge the financial support for the work to the Ministry of Economy and Competitiveness of Spain under the Project DPI2011-25999.

References

[1] Pecata O, Rentscha R, Brinksmeier E. Influence of milling process parameters on the surface integrity of CFRP. Proc CIRP 2012;1:466–70.

[2] Santiuste C, Barbero E, Miguélez MH. Computational analysis of temperature effect in composite bolted joints for aeronautical applications. J Reinf Plast Compos 2011;30(1):3–11.

[3] Davim JP, Reis P, Conceição C. Drilling fiber reinforced plastics (FRP) manufactured by hand-layup influence of matrix (VIAPAL VUP 9731 and ATLAC 382-05). J Mater Process Technol 2004;155–156:1828–33.

[4] Abrao AM, Campus Rubio J, Faria PE, Davim JP. The effect of cutting tool geometry on thrust force and delamination when drilling glass fiber reinforced plastic composite. Mater Des 2008;29(2):508–13.

[5] Davim P, Campos Rubio J, Abrao AM. A novel approach based on digital analysis to evaluate the delamination factor after drilling composite laminates. Compos Sci Technol 2007;67(9):1939–45.
[6] Rubio JC, Abrao A, Faria P, Esteves Correia A, Davim JP. Effects of high speed in the drilling of glass fiber reinforced plastic: evolution of the delamination factor. Int J Mach Tools Manuf 2008;48:715–20.
[7] DeFu L, Yong Jun T, Cong WL. A review of mechanical drilling for composite laminates. Compos Struct 2012;94:1265–79.
[8] Ramesh MV, Seetharamu KN, Ganesan N. Analysis of machining of FRPs using FEM. Int J Mach Tools Manuf 1998;38:1531–49.
[9] Mahdi M, Zhang L. A finite element model for the orthogonal cutting of fiber reinforced composite materials. J Mater Process Technol 2001;113:373–7.
[10] Iliescu D, Gehin D, Iordanoff I, et al. A discrete element method for the simulation of CFRP cutting. Compos Sci Technol 2010;70:73–80.
[11] Santiuste C, Soldani X, Miguélez H. Machining FEM model of long fiber composites for aeronautical components. Compos Struct 2010;92:691–8.
[12] Soldani X, Santiuste C, Muñoz-Sánchez A, Miguélez H. Influence of tool geometry and numerical parameters when modelling orthogonal cutting of LFRP composites. Compos A Appl Sci Manuf 2011;42:1205–16.
[13] Santiuste C, Miguélez H, Soldani X. Out-of-plane failure mechanisms in LFRP composite cutting. Compos Struct 2011;93:2706–13.
[14] Santiuste C, Olmedo A, Soldani X, Miguélez H. Delamination prediction in orthogonal machining of carbon long fiber-reinforced polymer composites. J Reinf Plast Compos 2012;31(13):875–85.
[15] Phadnis VA, Makhdum F, Roy A, Silberschmidt VV. Drilling in carbon/epoxy composites: experimental investigations and finite element implementation. Compos A Appl Sci Manuf 2013;47:41–51.
[16] Isbilir O, Ghassemieh E. Numerical investigation of the effects of drill geometry on drilling induced delamination of carbon fiber reinforced composites. Compos Struct 2013;105:126–33.
[17] Durão LMP, Gonçalves DJS, Tavares JMRS, Albuquerque VH, Aguiar Vieira A, Torres Marques A. Drilling tool geometry evaluation for reinforced composite laminates. Compos Struct 2010;92:1545–50.
[18] Durão LMP, de Moura MFSF, Marques AT. Numerical prediction of delamination onset in carbon/epoxy composites drilling. Eng Fract Mech 2008;75:2767–78.
[19] Durão LMP, de Moura MFSF, Marques AT. Numerical simulation of the drilling process on carbon/epoxy composite laminates. Compos A Appl Sci Manuf 2006;37:1325–33.
[20] Singh N, Bhatnagar N, Viswanath P. Drilling of uni-directional glass fiber reinforced plastics: experimental and finite element study. Mater Des 2008;29:546–53.
[21] Chinmaya M, Dandekar R, Shin YC. Modeling of machining of composite materials: a review. Int J Mach Tools Manuf 2012;57:102–21.
[22] Hibbit, Karlson, Sorensen Inc. ABAQUS user's manual 6.4-1; 2003.
[23] Hou JP, Petrinic N, Ruiz C, Hallett SR. Prediction of impact damage in composite plates. Compos Sci Technol 2000;60(2):273–81.
[24] Santiuste C, Sánchez-Sáez S, Barbero E. A comparison of progressive-failure criteria in the prediction of the dynamic bending failure of composite laminated beams. Compos Struct 2010;92(10):2406–14.
[25] López-Puente J, Zaera R, Navarro C. Experimental and numerical analysis of normal and oblique ballistic impacts on thin carbon/epoxy woven laminates. Compos A Appl Sci Manuf 2008;39(2):374–87.
[26] Fish JC, Lee SW. Delamination of tapered composite structures. Eng Fract Mech 1989;34(1):43–54.
[27] Benzeggagh ML, Kenane M. Measurement of mixed-mode delamination fracture toughness of unidirectional glass/epoxy composites with mixed mode bending apparatus. Compos Sci Technol 1996;56:439–49.
[28] Camanho PP, Davila CG. Mixed-mode decohesion finite elements for the simulation of delamination in composite materials. NASA/TM-2002-211737; 2002. p. 1–37.
[29] Olmedo A, Santiuste C. On the prediction of bolted single-lap composite joints. Compos Struct 2012;94:2110–7.
[30] Varas D, Artero-Guerrero JA, Pernas-Sánchez J, López-Puente J. Analysis of high velocity impacts of steel cylinders on thin carbon/epoxy woven laminates. Compos Struct 2013;95:623–9.